PROTEINS
STRUCTURE ■ FUNCTION ■ BIOINFORMATICS

Structural thermodynamics of protein preferential solvation: Osmolyte solvation of proteins, aminoacids, and peptides

Matthew Auton, D. Wayne Bolen, and Jörg Rösgen*

Department of Biochemistry and Molecular Biology, University of Texas Medical Branch, Galveston, Texas 77555-1052

ABSTRACT

Protein stability and solubility depend strongly on the presence of osmolytes, because of the protein preference to be solvated by either water or osmolyte. It has traditionally been assumed that only this relative preference can be measured, and that the individual solvation contributions of water and osmolyte are inaccessible. However, it is possible to determine hydration and osmolyte solvation (osmolation) separately using Kirkwood-Buff theory, and this fact has recently been utilized by several researchers. Here, we provide a thermodynamic assessment of how each surface group on proteins contributes to the overall hydration and osmolation. Our analysis is based on transfer free energy measurements with model-compounds that were previously demonstrated to allow for a very successful prediction of osmolyte-dependent protein stability. When combined with Kirkwood-Buff theory, the Transfer Model provides a space-resolved solvation pattern of the peptide unit, amino acids, and the folding/unfolding equilibrium of proteins in the presence of osmolytes. We find that the major solvation effects on protein side-chains originate from the osmolytes, and that the hydration mostly depends on the size of the side-chain. The peptide backbone unit displays a much more variable hydration in the different osmolyte solutions. Interestingly, the presence of sucrose leads to simultaneous accumulation of both the sugar and water in the vicinity of peptide groups, resulting from a saccharide accumulation that is less than the accumulation of water, a net preferential exclusion. Only the denaturing osmolyte, urea, obeys the classical solvent exchange mechanism in which the preferential interaction with the peptide unit excludes water.

Proteins 2008; 73:802–813.

Key words: transfer model; Kirkwood-Buff theory; osmolytes; protein folding; preferential interaction.

INTRODUCTION

Proteins are indispensable for life, and in view of the large variability of environmental conditions that living organisms face it is amazing how sensitively these macromolecules respond to changes in their environment. Cells, or whole organisms are exposed to potentially harmful fluctuations in temperature, pressure, and solution composition. To counteract these cellular stresses, virtually all organisms are equipped with osmolytes to protect their cells.[1,2] Cellular osmolytes are normally organic, though some archaea use salt instead.

The impact of naturally occurring osmolytes on protein conformational stability has been studied for a long time. The denaturing osmolyte, urea, has been the prime research object for many years,[3,4] but later attention was drawn also to the dependence of protein thermodynamics on protecting osmolytes.[5,6] Despite early attempts to predict osmolyte-dependent protein stabilities,[7] such predictions have only very recently become successful.[8–10] Before, analysis of osmolyte effects on proteins were limited to investigating whole proteins. Now, it is possible to resolve the structural details of the energetic effects on the protein surface, and to understand the contribution of each chemical group on the protein to its response to osmolytes. In this study, we pursue the latter approach and analyze the origin of the osmolyte-dependent protein energetics on a per-residue basis.

There are two major approaches in analyzing the effects of osmolytes on proteins. The classical heuristic approach implements model assumptions to derive solvation information from the experimental thermodynamic data.[11–14] A rigorous statistical mechanic approach was only implemented recently. It is based on Kirkwood-Buff theory,[15] which established a procedure of calculating a wealth of thermodynamic information from the structure of the solution, as given by radial distribution functions. These functions are similar to the angle-dependent radial distribution functions that define crystal structures. In solution, however, the molecules move and tumble, and so the structure of a solution is normally given in

Matthew Auton's current address is Department of Bioengineering Rice University Houston, Texas 77005-1892.
Grant sponsor: NIH/NIGMS; Grant number: R01GM049760.
*Correspondence to: Jörg Rösgen, Department of Biochemistry and Molecular Biology, University of Texas Medical Branch, Galveston, TX 77555-1052. E-mail: jorosgen@utmb.edu
Received 29 February 2008; Accepted 3 April 2008
Published online 22 May 2008 in Wiley InterScience (www.interscience.wiley.com).
DOI: 10.1002/prot.22103

Table I
Osmolyte Solution Properties at 25°C

1*M* osmolyte	MW	ρ (g/mL)	c_1 (mol/L)	$\bar{v}_3$ (mL/mol)[a]	$\bar{v}_1$ (mL/mol)	$(\partial\mu_3/\partial \ln c_3)/RT$[b]
Water	18.02	0.9970429	55.34		18.07	
TMAO	75.11	0.999587	51.30	71.2 ± 0.2	18.10	1.51351
Sarcosine	89.10	1.022429	51.79	66.7 ± 0.2	18.02	1.13021
Betaine	117.15	1.01579	49.87	98.25 ± 0.06	18.08	1.50457
Proline	115.10	1.029823	50.76	85.3 ± 0.2	18.02	1.19877
Glycerol	92.09	1.018795	51.43	72.71 ± 0.08	18.03	1.10756
Sorbitol	182.17	1.059932	48.71	123.0 ± 0.2	18.00	1.18265
Sucrose	342.30	1.12687	43.54	214.6 ± 0.4	18.04	1.57121
Trehalose	342.30	1.134137	43.94	215.9 ± 0.7	17.84	1.69395[c]
Urea	60.06	1.012838	52.87	45.24 ± 0.08	18.06	0.97147
2*M* sarcosine	89.10	1.046896	48.21	66.7 ± 0.2	17.97	0.64970
0.5*M* sucrose	342.30	1.061635	49.42	214.6 ± 0.4	18.06	2.45646
2*M* urea	60.06	1.028288	50.40	45.24 ± 0.08	18.05	0.48170

[a]Errors on the partial volume of osmolyte, $\bar{v}_3$, are representative fitting errors.
[b]Calculated from parameters in Table 1 of Ref. 34 and equations therein at 1*M* osmolyte or the indicated molarity.
[c]Calculated from Table 1 of Ref. 35.

terms of angle-averaged radial distribution functions. The original Kirkwood-Buff theory derived thermodynamics from structure. Ben-Naim showed that it is conversely possible to obtain structural information from thermodynamics.[16] After Ben-Naim's pioneering work[16,17] it took some decades before these principles were recognized in protein research, where Smith[18–26] and Shimizu[27–31] began popularizing Kirkwood-Buff theory.

In the following, we use Kirkwood-Buff theory and transfer free energies to first analyze the hydration and osmolyte-solvation (hereafter referred to as osmolation) of protein building blocks—amino acids and peptide backbone. After that we proceed to discuss the solvation of proteins in osmolyte solutions.

MATERIALS

Amino acids and osmolytes

All amino-acids and the osmolytes glycine-betaine, L-proline, glycerol, D-sorbitol, D-(+)-sucrose, and D-(+)-trehalose with purity above 99% were purchased from Sigma Chemical Co. Sarcosine was purchased from Fluka and ultrapure urea was purchased from ICN. All the purchased amino acids and osmolytes, with the exception of sarcosine, were used without further purification. Sarcosine was dissolved in water, cleaned with activated charcoal and recrystallized once from water. Trimethylamine-*N*-oxide (TMAO) was synthesized as described by Russo *et al.*[32]

Peptide backbone model compounds

N-acetyl triglycinamide (NAG_3A) and *N*-acetyl tetraglycinamide (NAG_4A) were synthesized as described in Ref. 33.

METHODS

Partial molar and apparent volumes

Osmolytes

The densities of osmolyte solutions, ρ (g/mL), over the full concentration range were determined at 25°C ± 0.002°C using an Anton Paar Densimeter DMA-602. Partial molar volumes of the osmolytes, $\bar{v}_3$, were determined from the slope of plots of the solution volume per kilogram of water as a function of osmolyte molality. $\bar{v}_3$ was found to be constant (density fits linear within ±0.06 to ±0.7 mL/mol) over a large range of concentration up to greater than 5*m* TMAO, 17*m* sarcosine, 6*m* betaine, 14*m* proline, 110*m* glycerol, 13*m* sorbitol, 3*m* sucrose, 2*m* trehalose, and 18*m* urea. The partial molar volume of water in the presence of c_3 molar osmolyte was calculated using the following equations.

$$\bar{v}_1 = \frac{1 - c_3\bar{v}_3}{c_1}. \quad (1)$$

where the molarity of water, c_1, at c_3 molar osmolyte is

$$c_1 = \frac{1000\rho - c_3 MW_3}{MW_1}. \quad (2)$$

In Eq. (2), MW_1 and MW_3 are the corresponding molecular weights of water and osmolyte. The densities of osmolyte solutions and the partial molar volumes of the osmolytes and water are reported in Table I.

Peptide backbone model compounds

Apparent volumes of NAG_3A and NAG_4A in water and 1*M* osmolyte were calculated from solubility data reported by Auton and Bolen.[33] The apparent molar

Table II
Apparent Volumes, $\overline{v}_{2,app}$ (mL/mol) of NAG_3A and NAG_4A and the Peptide Unit in 1*M* Osmolyte Solutions at 25°C

			Peptide unit
Osmolyte	NAG_3A	NAG_4A	$NAG_4A - NAG_3A$
Water	165.2	208.7	43.5
TMAO	161.1	180.5	19.4
Sarcosine	161.3	161.5	−0.2
Betaine	161.2	179.0	17.8
Proline	165.4	247.1	81.7
Glycerol	164.4	205.5	41.1
Sorbitol	164.0	225.1	61.1
Sucrose	152.7	56.1	−96.6
Trehalose	160.0	135.9	−23.9
Urea	163.7	200.3	36.7

volume of the model compound, $\overline{v}_{2,app}$, is determined as the difference in volume per kilogram of principle solvent between the saturated peptide solution and the osmolyte solution divided by the peptide molal solubility. The apparent molar volume of the peptide unit is calculated as the difference between the apparent molar volumes of NAG_4A and NAG_3A. Apparent volumes of NAG_3A, NAG_4A, and the peptide unit in 1*M* osmolytes are reported in Table II.

Amino acids

Apparent volumes of the amino acids in water, 1*M* TMAO, 2*M* sarcosine, 1*M* proline, 0.5*M* and 1*M* sucrose, and 2M urea were calculated from the solubility data reported in Refs. 8 and 36–38. Apparent volumes of the amino acids in 1*M* betaine, 1*M* glycerol, 1*M* sorbitol, and 1*M* trehalose were calculated from solubility data determined in our laboratory in the process of measuring transfer free energies of the amino acids from water to these osmolytes.[8] The amino acid apparent volume, $\overline{v}_{2,app}$, is determined as the difference in volume per kilogram of principle solvent between the saturated amino acid solution and the osmolyte solution divided by the amino acid molal solubility. The apparent volumes of amino acids in water are generally in good agreement with the reported partial molar volumes at infinite dilution[39] (see Table III), indicating that the first order assumption of a linearly concentration dependent solution density is satisfactory. All of the apparent volumes of amino acids are reported in Table III.

Transfer free energies

Peptide backbone unit

Transfer free energies of the peptide unit from water to 1*M* osmolytes were obtained using the constant increment values of the *N*-acetyl glycinamide series of peptides given in Table 2 of Ref. 33.

Amino acids

Amino acid transfer free energies from water to 1*M* TMAO, 2*M* sarcosine, 1*M* proline, 0.5*M* and 1*M* sucrose, and 2*M* urea were obtained from Refs. 8 and 36–38. Transfer free energies of amino acids from water to 1*M*

Table III
Amino Acid Apparent Volumes, $\overline{v}_{2,app}$ (mL/mol) in Osmolyte Solutions at 25°C

Amino acid	Water[a]	1*M* TMAO	2*M* sarcosine	1*M* betaine	1*M* proline	1*M* glycerol	1*M* sorbitol	0.5*M* sucrose	1*M* sucrose	1*M* trehalose	2*M* urea
Nonpolar											
Ala	61.73 (60.54 ± 0.07)	61.50	62.42	61.20	62.72	61.80	62.36	61.51	61.63	62.35	62.82
Phe	116.19 (121.5 ± 0.2)	119.34	102.71	120.78	126.01	117.44	124.31	118.08	115.12	130.07	123.38
Leu	107.60 (107.77 ± 0.05)	104.98	102.56	106.59	112.62	107.77	108.61	102.55	94.44	115.72	109.25
Ile	105.66 (105.80 ± 0.07)	105.10	102.06	104.07	109.60	104.14	107.09	102.68	97.80	99.71	106.47
Val	90.73 (90.75 ± 0.10)	89.83	90.01	90.80	103.27	93.51	91.82	89.63	87.31	88.25	91.85
Pro	85.86 (82.76 ± 0.10)	85.46	85.93	85.93	86.33	86.81	85.89	86.33	85.80	86.13	86.44
Met	105.24 (105.57 ± 0.02)	104.02	104.53	104.19	108.69	106.02	107.22	104.41	101.84	103.34	105.94
Polar											
Gly	45.51 (43.26 ± 0.07)	45.41	46.77	45.95	46.48	46.33	46.58	45.77	46.11	46.65	46.40
Ser	64.63 (60.62 ± 0.05)	63.87	65.58	64.50	65.08	64.00	64.82	65.36	64.14	65.01	64.71
Thr	77.69 (76.90 ± 0.10)	77.44	78.36	76.89	79.47	77.87	78.52	77.30	76.69	77.55	79.02
Gln	93.76 (NR)	93.69	92.57	92.82	98.02	95.44	94.99	93.10	89.98	89.75	98.02
Asn	81.50 (78.0 ± 0.5)	77.78	77.15	76.30	83.22	78.36	79.37	76.21	69.59	69.24	116.82
Acidic											
Asp	75.90 (74.8 ± 0.2)	75.56	78.25	84.02	84.79	85.13	86.33	77.92	79.24	85.69	77.29
Glu	89.57 (89.85 ± 0.1)	90.80	92.71	96.84	98.34	97.43	98.93	92.01	93.65	98.82	92.08
Basic											
His	99.62 (98.3 ± 0.1)	98.44	97.92	99.41	102.80	100.36	100.07	96.59	95.83	96.59	102.10
Lys	132.13 (108.5)	132.03	135.09	88.41	133.68	133.12	134.02	134.28	164.35	132.80	133.50
Arg	147.16 (127.42 ± 0.01)	147.97	149.81	147.25	148.15	147.77	148.71	148.53	150.05	148.63	147.94

[a]The partial molar volumes, $\overline{v}_2$, of amino acids in water at infinite dilution published in Ref. 39 are noted in parentheses of column 2.
NR indicates "not reported."

Table IV
Amino Acid Intrinsic Transfer Free Energies, $\Delta\overline{G}^{\circ}_{tr,int}$ (cal/mol), in Osmolyte Solutions at 25°C

Amino acid	1*M* TMAO	2*M* sarcosine	1*M* betaine	1*M* proline	1*M* glycerol	1*M* sorbitol	0.5*M* sucrose	1*M* sucrose	1*M* trehalose	2*M* urea
Nonpolar										
Ala	169.15	177.89	183.25	121.92	76.55	108.32	118.05	238.15	250.62	36.36[a]
Phe	174.46	130.78	65.55	50.73	128.56	126.91	89.80	119.74	199.49	−110.52
Leu	195.41	232.72	160.75	126.76	34.37	143.69	126.21	253.20	313.55	−53.43
Ile	158.35	236.02	177.21	119.27	105.02	145.31	114.58	244.22	297.03	−21.15
Val	182.77	214.71	158.85	129.95	67.42	130.36	120.04	250.01	314.16	12.39
Pro	46.06	87.60	53.32	58.03	8.24	66.31	73.09	143.07	122.70	20.40
Met	176.14	172.42	164.32	86.87	82.66	111.96	104.25	209.43	246.56	−40.98
Polar										
Gly	183.79	156.07	178.48	121.99	68.79	90.30	105.49	216.09	217.37	20.69[a]
Ser	144.74	100.10	136.63	88.50	75.10	86.44	102.64	213.31	216.39	14.58
Thr	187.36	140.99	178.81	103.66	86.32	111.01	114.94	236.91	243.69	11.52
Gln	225.20	135.69	186.05	89.73	66.03	71.75	87.78	175.22	181.03	−53.92
Asn	239.48	74.20	211.65	104.28	120.36	69.78	119.16	187.82	266.04	−21.87
Acidic										
Asp	117.12	127.66	61.92	31.48	−16.67	14.28	86.03	178.92	120.83	62.79
Glu	100.53	130.85	66.41	32.82	−5.41	27.20	82.80	174.44	131.45	56.93
Basic										
His	225.86	114.47	142.51	76.89	51.62	48.53	50.94	97.43	118.62	−45.32
Lys	73.56	101.22	6.50	62.12	34.78	68.75	88.02	176.49	167.30	10.19
Arg	74.52	91.59	69.04	61.81	38.05	71.45	88.79	136.78	167.04	13.36

The concentration scale correction factor, $\Delta\overline{G}^{\circ}_{SC,\infty}$, is given in Table 1 of Ref. 33 for 1*M* osmolyes. For 2*M* sarcosine, 0.5*M* sucrose, and 2*M* urea, $\Delta\overline{G}^{\circ}_{SC,\infty}$, is −28.90, −37.19, and −18.28 (cal/mol), respectively, on the molarity scale.
[a]The transfer free energies reported for glycine and alanine in 2*M* urea are actual transfer chemical potentials as the glycine and alanine activity coefficients in water and 2*M* urea have been accounted for as described by Auton *et al.*[10]

betaine, 1*M* glycerol, and 1*M* sorbitol were obtained from the online supplement of Ref. 8. The transfer free energies were adjusted by a molar concentration scale correction free energy as described by Auton and Bolen using the values reported in Table 1 of Ref. 33 for 1*M* osmolytes and −28.90, −37.19, and −18.28 (cal/mol), respectively, for 2*M* sarcosine, 0.5*M* sucrose, and 2*M* urea. All of the amino acid transfer free energies are reported on the molar scale in Table IV.

Proteins

A database of 36 proteins was used to calculate predicted *m*-values using transfer free energies from water to 1*M* osmolyte. The transfer free energy difference between native and denatured in 1*M* osmolyte was calculated from amino acid side chain and peptide unit transfer free energy data weighted according to the average fractional change in solvent accessibility for each residue in the protein. Native state accessibility was determined using Lee and Richards algorithm as modified by Lesser and Rose.[40,41] Schellman's model was used for calculating the denatured state accessibility taken as an average between the compact and fully extended models decribed by Creamer *et al.*[42–44] The 36 proteins used in our database were obtained from the supplement of Auton *et al.*[10] and were selected based on the following criteria. Proteins are monomeric, unliganded, and exhibit two-state urea denaturation in the pH range of 6–8 and temperatures between 20 and 40°C.

Estimation of contact volumes

Osmolyte probe radii were calculated assuming a spherical geometry from the molecular volumes determined from the osmolyte crystal coordinates[45–53] in the Cambridge Structure Database[54] using the program STERIC.[55] The used probe radii in Å were 1.4 (water), 2.33 (urea), 2.66 (TMAO), 2.69 (sarcosine), 2.74 (glycerol), 2.94 (proline), 2.98 (glycine betaine), 3.32 (sorbitol), 3.98 (sucrose), and 4.01 (trehalose). The mutual contact volumes of the peptide unit with water and the osmolytes were estimated to obtain an approximate measure of the contribution of immediate steric exclusion to the Kirkwood-Buff integrals, that is, integration between 0 and contact distance. Contact volumes were calculated using the program MOLMOL.[56] A linear stretch of 10 amino acids was selected (from 1gb1), and the volume of increasing lengths *n* (from 3 to 10 amino-acids) of peptide backbone was determined. The slope of volume versus *n* was taken as contact volume of a peptide unit.

THEORY

In this section, we give a brief overview of how to calculate solvation behavior from experimental data. For this purpose, we discuss the experimental *m*-value, how

it can be predicted using the transfer model, and finally the calculation of solvation parameters from these measured and/or predicted experimental data. The hydration and osmolation information is extracted using Kirkwood-Buff theory.[15] We discuss three-component systems containing water (component 1), the (poly-) peptide or amino acid solute (component 2), and osmolyte (component 3). We restrict the discussion to the case of dilute component 2, the solute.

m-values

In a two-state equilibrium, the free energy change for the $N \rightarrow D$ conversion, $\Delta G^{c_3}_{N \rightarrow D}$, is usually assumed to be a linear function of osmolyte molarity, c_3. This has been demonstrated for urea,[3] and is also valid for some protecting osmolytes.[57–59] This linearity allows for application of the linear extrapolation method (LEM).[3,60,61]

$$\Delta G^{c_3}_{N\rightarrow D} = \Delta G^{0M}_{N\rightarrow D} + mc_3. \qquad (3)$$

The slope, m, is a measure of the cooperativity of the transition, and the intercept, $\Delta G^{0M}_{N\rightarrow D}$, represents the $N \rightarrow D$ free energy change in the absence of osmolyte. Since $\Delta G = -RT \ln K$, the m-value is the derivative of the natural log of the equilibrium constant for $N \rightleftharpoons D$ with respect to the molarity of osmolyte

$$\frac{m}{RT} = -\left(\frac{\partial \ln K}{\partial c_3}\right)_{T,p,c_2}. \qquad (4)$$

Transfer free energies

Recently, we have shown that transfer free energies of amino acid side chains and the peptide backbone can be used to quantitatively predict the m-value,[8,10] which implies that the transfer free energies are additive.[33] The thermodynamic cycle in the Transfer Model (Fig. 1) indicates that the difference between the free energies of unfolding in the presence and absence of osmolyte, $\Delta G^{1M}_{N\rightarrow D} - \Delta G^{0M}_{N\rightarrow D}$, is equal to the free energy difference of transfering N and D from dilute buffer to a solution of $1M$ osmolyte, $\Delta G^{0\rightarrow 1M}_{\mathrm{tr},D} - \Delta G^{0\rightarrow 1M}_{\mathrm{tr},N}$. Referring back to the LEM, Eq. (3), at $c_3 = 1M$ osmolyte the difference between denatured and native state transfer free energies is equal to the m-value

$$m \cdot 1M = \Delta G^{1M}_{N\rightarrow D} - \Delta G^{0}_{N\rightarrow D} = \Delta G^{0\rightarrow 1M}_{\mathrm{tr},D} - \Delta G^{0\rightarrow 1M}_{\mathrm{tr},N}, \qquad (5)$$

or, at osmolyte concentration c_3,

$$m \cdot c_3 = \Delta G^{c_3}_{N\rightarrow D} - \Delta G^{0}_{N\rightarrow D} = \Delta G^{0\rightarrow c_3}_{\mathrm{tr},D} - \Delta G^{0\rightarrow c_3}_{\mathrm{tr},N}. \qquad (6)$$

This difference in transfer free energies between denatured and native is obtained by summing the individual transfer free energies of the amino acid side chains and the peptide backbone

$$\Delta G^{0\rightarrow 1M}_{\mathrm{tr},D} - \Delta G^{0\rightarrow 1M}_{\mathrm{tr},N} = \sum_{j=1}^{n} \Delta g_{\mathrm{tr},j,sc}\Delta\alpha_{j,\mathrm{sc}} + \Delta g_{\mathrm{tr,bb}} \sum_{j=1}^{n} \Delta\alpha_{j,\mathrm{bb}}. \qquad (7)$$

Here, $\Delta\alpha_j$ is the difference in the average fractional exposure between N and D of either the peptide backbone unit or the amino acid side chain of residue number j, $\Delta g_{\mathrm{tr,bb}}$ is the transfer free energy of the peptide backbone unit described in Auton and Bolen,[33] and $\Delta g_{\mathrm{tr},j,\mathrm{sc}}$ is the transfer free energy of an amino acid side chain of type j.[8] Both of these refer to a transfer from water to $1M$ osmolyte.

In general, the transfer free energy of a solute from water to c_3 molar osmolyte, $\Delta G^{c_3}_{\mathrm{tr}}$, could depend on the osmolyte concentration in a non linear manner. There is some evidence, however, that transfer free energies change linearly with c_3. First, the difference between native and denatured state transfer [Eq. (6)] is linear. Second, according to the transfer data from water to 2, 4, and $6M$ sarcosine and to 0.5 and $1M$ sucrose reported by Liu and Bolen,[26] the transfer free energies of many of the side chains are linear as a function of osmolyte concentration. The transfer free energies of amino acid side chains to different concentrations of urea are also linear as a function of urea concentration.[7,62] Therefore, the transfer free energy can be expressed in terms of the derivative of the solute chemical potential μ_2 with respect to the osmolyte molarity c_3

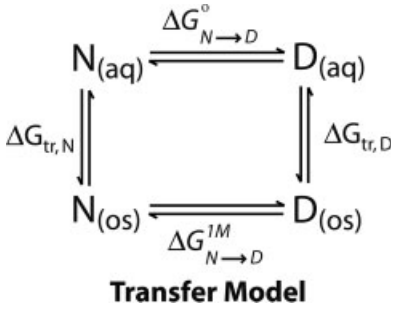

Figure 1

Thermodynamic cycle of the Transfer Model. The horizontal equilibria are denaturation in the absence (top) and presence (bottom) of $1M$ osmolyte. The vertical equilibria are the transfer from water to $1M$ osmolyte of the native (left) and denatured state (right). Note that in this cycle the relation $\Delta G^{1M}_{N\rightarrow D} - \Delta G^{0}_{N\rightarrow D} = \Delta G^{0\rightarrow 1M}_{\mathrm{tr},D} - \Delta G^{0\rightarrow 1M}_{\mathrm{tr},N}$ holds.

$$\frac{\Delta G_{\mathrm{tr}}^{0\to 1M}}{(1M)} = \frac{\Delta G_{\mathrm{tr}}^{0\to c_3}}{c_3} = \left(\frac{\partial \mu_2}{\partial c_3}\right)_{T,p,c_2} \tag{8}$$

This first equality is valid, because of the linearity of $\Delta G_{\mathrm{tr}}^{0\to c_3}$. The ratio $\Delta G_{\mathrm{tr}}^{0\to c_3}/c_3$ is then a secant, $\Delta G_{\mathrm{tr}}^{0\to c_3}/\Delta c_3 = \Delta\mu_2/\Delta c_3$, where $\Delta\mu_2 = \mu_2^{c_3} - \mu_2^{0M}$ and $\Delta c_3 = c_3 - 0M = c_3$. Because of the linearity, this secant equals the derivative $\partial\mu_2/\partial c_3$.

Kirkwood-Buff theory

Kirkwood-Buff (KB) theory provides a link between structure and thermodynamics of solutions, and is based on first principles of statistical mechanics.[15] Within the KB framework, the structure around Component 2 is expressed in terms of pair correlation functions h_{2i}, which are a measure of the deviation from random distribution of particles of type i around Component 2. The overall correlation, or KB parameter, $\mathcal{G}_{2i}$, is defined as the excess solvation of component i, water or osmolyte, around Component 2, which could be, for example, a protein. The KB parameters are obtained by integrating $h_{2i}(r)$

$$\mathcal{G}_{2i} = \int h_{2i}(r) 4\pi r^2 \mathrm{d}r \tag{9}$$

The $\mathcal{G}_{2i}$ can be expressed in terms of experimental thermodynamic properties using the expressions[25,63]

$$-\bar{v}_2 = c_1\bar{v}_1\mathcal{G}_{21} + c_3\bar{v}_3\mathcal{G}_{23} \tag{10}$$

and[64]

$$\left(\frac{\partial \mu_2}{\partial c_3}\right)_{T,p} = (\mathcal{G}_{21} - \mathcal{G}_{23})\left(\frac{\partial \mu_3}{\partial \ln c_3}\right)_{T,p}. \tag{11}$$

These two equations can be solved for the two unknowns $\mathcal{G}_{21}$ and $\mathcal{G}_{23}$. Using Eq. (8) results then in

$$\mathcal{G}_{21} = -\bar{v}_2 + \phi_3 \frac{\Delta G_{\mathrm{tr}}^{0\to 1M}}{(\partial\mu_3/\partial \ln c_3)} \tag{12}$$

$$\mathcal{G}_{23} = -\bar{v}_2 + (\phi_3 - 1)\frac{\Delta G_{\mathrm{tr}}^{0\to 1M}}{(\partial\mu_3/\partial \ln c_3)}, \tag{13}$$

where $\phi_3 = c_3\bar{v}_3$ is the volume fraction of Component 3. Expressing these equations in terms of m-values is possible considering the change of $\mathcal{G}_{21}$ and $\mathcal{G}_{23}$ upon unfolding[64]

$$\Delta_N^D\mathcal{G}_{21} = -\Delta_N^D\bar{v}_2 + \phi_3\frac{m}{(\partial\mu_3/\partial \ln c_3)} \tag{14}$$

$$\Delta_N^D\mathcal{G}_{23} = -\Delta_N^D\bar{v}_2 + (\phi_3 - 1)\frac{m}{(\partial\mu_3/\partial \ln c_3)}. \tag{15}$$

Though the m-value is accessible more easily, the transfer model allows for a space-resolved prediction of energetic contributions to stability of all chemical groups on the protein surface.[8] Similar equations have been reported previously also for preferential interaction parameters in place of the m-value or transfer free energy.[63]

In the following, we will apply KB theory to both experimental data and predicted transfer free energies to obtain solvation information on amino acids, peptides, and proteins.

RESULTS AND DISCUSSION

Solvation of the peptide backbone

To calculate the hydration and the osmolation of the backbone, we use Eqs. (12) and (13). Three experimental properties are required for this calculation: the transfer free energy of the peptide unit $\Delta G_{\mathrm{tr}}^{0\to 1M}$ (given in Table 2 of Ref. 33), the partial molar volumes of the peptide unit $\overline{v}_2$ (given here in Table II), and $(\partial\mu_3/\partial c_3)$ (given in Table I). Figure 2 shows the hydration and osmolation of the peptide unit in $1M$ osmolyte.

Methylamines, proline, and polyols: osmolyte exclusion

In Figure 2, the osmolytes are grouped according to their peptide unit solvation behavior. The methylamines, TMAO, sarcosine, and betaine show very little change in the hydration, $\mathcal{G}_{21}$, of the peptide unit upon transfer from water to $1M$ osmolyte (gray bar), however the

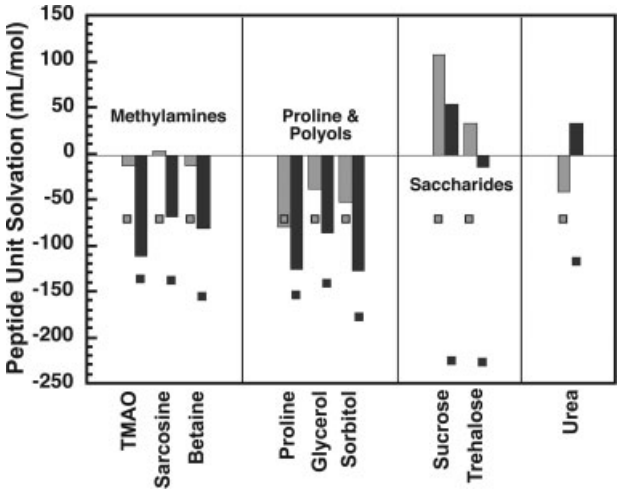

Figure 2

Kirkwood-Buff integrals for the hydration, $\mathcal{G}_{21}$ (gray), and osmolation, $\mathcal{G}_{23}$ (black), of the peptide backbone unit. The difference, $\mathcal{G}_{23} - \mathcal{G}_{21}$, provides a measure of the preferential interaction, which is negative for protecting osmolytes (exclusion) and positive for urea (accumulation). The squares indicate approximate values for mutual contact volumes of a peptide unit with water (gray) (−70 mL/mol), and each of the osmolytes (black).

osmolation, $\mathcal{G}_{23}$ (black bar), is large and negative. This indicates that the methylamines are strongly excluded from the peptide unit. The net-zero effect with respect to the number of water molecules is significant. An exclusion of water from the backbone moiety would be expected because water and peptide cannot overlap. The lack of exclusion thus indicates that the water density at the surface of the peptide group must be increased relative to the bulk. Therefore, to some extent, the exclusion of osmolyte could be viewed as a direct consequence of the increased number of water molecules around the peptide group that occupy the available space. However, as discussed later, the osmolyte might actually be considered to be accumulated around the peptide group—relative to simple steric exclusion between water and peptide backbone.

The amino acid proline and the polyols, glycerol, and sorbitol also are strongly excluded from the peptide unit, but in the presence of these osmolytes also a large amount of water is excluded from the peptide unit.

Saccharides and urea: accumulation of osmolyte

The saccharides, sucrose, and trehalose, exert their effects differently than do the other protecting osmolytes (Fig. 2). These osmolytes favorably interact with the peptide unit. Concomitantly, the peptide unit becomes excessively hydrated. The net effect of trehalose is a large hydration of the peptide unit with a net-zero solvation by trehalose. Sucrose is even more enriched around peptide groups. Along with the additional positive hydration, this enrichment causes the local density of the solution to strongly increase around the peptide unit. In fact, the positive solvation of the peptide unit by sucrose is comparable with the enrichment of urea around the peptide unit. Sucrose, however, brings additional waters of hydration to the peptide unit, whereas urea excludes waters of hydration.

Net preferential interaction

The difference between $\mathcal{G}_{23}$ and $\mathcal{G}_{21}$ is a measure of the preferential interaction between osmolyte and the peptide unit. Eventhough all the protecting osmolytes exhibit a preferential exclusion around the peptide unit, this arises for very different reasons depending on how each osmolyte solvates and hydrates the backbone. The large overall unfavorable interaction (preferential exclusion) between methylamines and the backbone[33] is simply due to osmolyte exclusion, and water plays only a small role, if any, in this interaction. For proline and the polyols, the unfavorable interaction is due to both water and osmolyte exclusion where the exclusion of osmolyte is greater than that of water. The solvation interaction of saccharides with the peptide backbone results in a accumulation of water that is greater than the accumulation of the sugar. The osmolyte, urea, is destabilizing because it accumulates around the peptide unit while water is simultaneously excluded, resulting in a solvent exchange.

How can these observations be interpreted in terms of the local structure of the solution, extending radially from the peptide unit? Radial distribution functions may be considered as composed of two contributions. First, the mere fact that molecules do not overlap leads to an exclusion, that is, a negative volume contribution, at short distances. For spherical molecules this holds up to the sum of the radii. Second, solvation shells form around this region of steric exclusion. Packing effects result in such solvation shells already by themselves, even in the absence of attractive interactions. Additional interactions will modify the solvation further through attraction or repulsion, so solvation shells can contribute either positively or negatively to the overall solvation $\mathcal{G}_{ij}$. Figure 2 illustrates the difference between the overall solvation (bars) and the immediate volume exclusion (squares), given by the contact volume.

Focusing first on the hydration, we see that the hydration of the peptide unit is qualitatively similar to the steric exclusion values only in solutions of polyols, proline, and urea (Fig. 2). In contrast, large positive deviations occur in the presence of both methylamines and saccharides. This enrichment of water is consistent with the normal occurrence of packing-related solvation peaks of higher density that are typical for highly concentrated solutions. However, the enrichment of water is large, especially in the case of the saccharides. Relative to the effects of steric exclusion, osmolytes appear to be generally accumulated around peptide backbone, though this effect is strong only for saccharides and urea.

Solvation of amino acids

We discuss the solvation of amino acids for two purposes. First, free amino acids are directly impacted by the high and fluctuating intracellular osmolyte concentrations that can occur during volume regulation and cellular osmotic control. Second, amino acids have been used as model compounds for side-chain contributions to the overall energetics of proteins[8,36–38,66,67] It has been pointed out that peptide model compounds may be preferable,[33,68–71] but such data are not yet available for transfer free energy calculations. Nevertheless, amino acids appear to be sufficiently good model compounds for our purposes of calculating protein stabilities in osmolyte solutions,[8,10] as used in the following section.

The solvation of amino acids can be calculated in the same way as that of the peptide backbone. Again, we use Eqs. (12) and (13) to calculate $\mathcal{G}_{21}$ and $\mathcal{G}_{23}$ for each amino acid. Amino acid apparent volumes and transfer free energies are given in Tables III and IV and the partial molar volume of the osmolyte is given in Table I. Figure 3

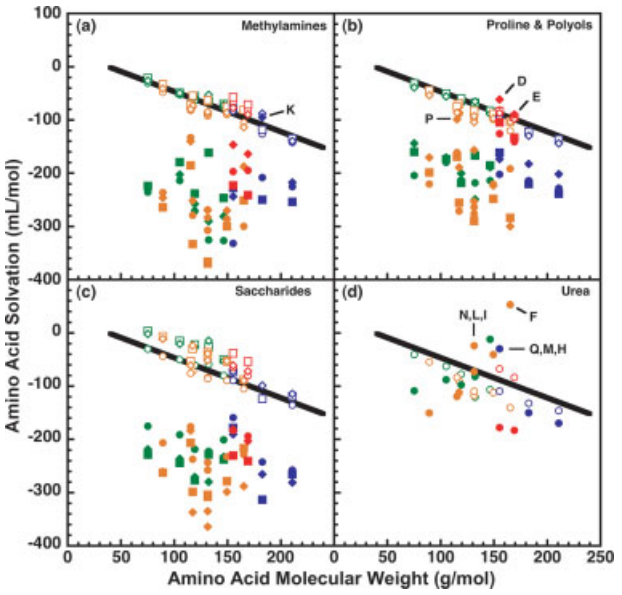

Figure 3

Kirkwood-Buff integrals for the hydration, $\mathcal{G}_{21}$ (open symbols), and osmolation, $\mathcal{G}_{23}$ (closed symbols), of amino acids at their solubility limit as a function of molecular weight. Panel (**a**): The methylamines, 1*M* TMAO ○s, 2*M* sarcosine □s, 1*M* betaine ◇s. Panel (**b**): proline and the polyols, 1*M* proline ○s, 1*M* glycerol □s, 1*M* sorbitol ◇s. Panel (**c**): The saccharides, 0.5*M* sucrose ○s, 1*M* sucrose □s, 1*M* trehalose ◇s. Panel (**d**): 2*M* urea ○s. The amino acids are color classified as nonpolar = orange, polar = green, acidic = red, and basic = blue. The solid line represents the average dependence of hydration, $\mathcal{G}_{21}$, on the size of the amino acid.

shows the hydration and osmolation of zwitterionic amino acids in osmolyte solutions as a function of the molecular weight of the amino acid. The figure is a composite of solvation parameters derived from our collection of transfer free energies, solubilities, and apparent volumes of amino acids in all of the osmolytes studied in our lab to date.[8,36–38] Data points in the figure represent the solvation of amino acids by all osmolytes, both protecting and nonprotecting, sorted according to the different osmolyte classes.

Figure 3 illustrates three important points. First, the variance in the hydration, $\mathcal{G}_{21}$, of amino acids is small when compared with the much larger variance in osmolation, $\mathcal{G}_{23}$. This indicates that the hydration of amino acids in one osmolyte solution is not very different from its hydration in another osmolyte solution regardless of the type of osmolyte present. The range is ~5 to −150 mL/mol. On the other hand, the osmolation of amino acids varies tremendously depending on the type of osmolyte in solution and can range approximately from 50 to −400 mL/mol. The scatter in the average osmolation is significantly greater than the scatter in the average hydration, $\mathcal{G}_{21}$. The solvation of the amino acids is different from one another primarily with respect to the amino-acid•osmolyte interactions that give rise to $\mathcal{G}_{23}$, and is strongly dependent upon both the type of amino acid and the type of osmolyte present.

Second, the hydration parameter, $\mathcal{G}_{21}$, is proportional to the amino acid molecular weight. Together with the observation that the variance in $\mathcal{G}_{21}$ is small from one type of osmolyte to another, this indicates that amino acid solvation by water in the presence of osmolyte is primarily determined by the size of the amino acid and the amount of space it occupies in solution.

Finally, solvation of all amino acids by water or osmolyte is negative and $\mathcal{G}_{23}$ is generally more negative than $\mathcal{G}_{21}$. This situation is similar to what is observed for the peptide unit in the presence of 1*M* proline, glycerol, and sorbitol in Figure 2. The net effect is that regardless of the osmolyte, free amino acids in solution exclude both osmolytes and water. The water, however, is excluded to a lesser degree, resulting in an overall preferential exclusion of the osmolyte. However, there are a few exceptions to this observation. In panels (a) and (b) of Figure 3, solvation of lysine by betaine, proline by sorbitol, and the acidic amino acids, aspartate and glutamate, by proline, glycerol, and sorbitol, $\mathcal{G}_{23}$, is very similar to the hydration, $\mathcal{G}_{21}$. For the nonprotecting osmolyte, urea, many of the amino acids in the mid-range of molecular weight have a urea solvation, $\mathcal{G}_{23}$, that is less negative than the hydration, $\mathcal{G}_{21}$. For these amino acids, asparagine, glutamine, leucine, isoleucine, methionine, phenylalanine, and histidine, urea preferentially solvates the amino acid while water is more excluded. An extreme example of this is phenylalanine in which $\mathcal{G}_{23}$ is positive.

Protein solvation

As discussed earlier in the Theory section, the Transfer Model provides a prediction of *m*-values, which have been shown to agree quite well with experimentally determined stabilities of several intrinsically unstructured proteins in osmolyte solution and for urea denaturation of stable proteins.[8,10] We have calculated the transfer free energy difference between the native and denatured states of a database of proteins using the method described earlier and Eqs. (14) and (15) to calculate the solvation differences between the native and denatured states in the presence of 1*M* osmolyte for water, $\Delta_N^D\mathcal{G}_{21}$, and osmolyte, $\Delta_N^D\mathcal{G}_{23}$. Since the partial molar volume change of the protein, $\Delta_N^D\overline{v}_2$, upon folding/unfolding is typically small, the majority of the solvation contribution will be contained in the second term of Eqs. (14) and (15). For this reason, $\Delta_N^D\overline{v}_2$ is typically neglected in the context of a Kirkwood-Buff treatment of protein folding. In fact, $\Delta_N^D\overline{v}_2$ is normally in the order of 2% or less than the protein volume,[72–75] and is thus expected to make a contribution that is of the size of the symbols in Figure 4.

Figure 4 illustrates some important properties about the solvation of proteins in 1*M* osmolyte solutions. In the figure, $\Delta_N^D\mathcal{G}_{21}$ is plotted versus $\Delta_N^D\mathcal{G}_{23}$ for our database of proteins. The proteins range in molecular weight

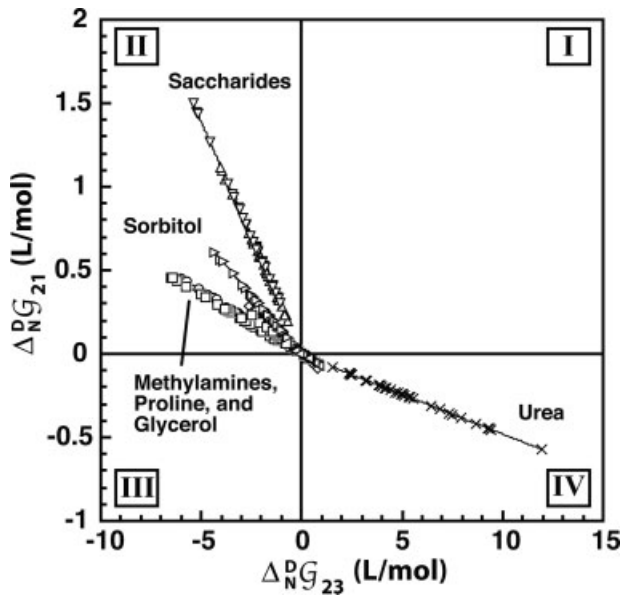

Figure 4

The change in hydration, $\Delta_N^D\mathcal{G}_{21}$, as a function of the change in osmolation, $\Delta_N^D\mathcal{G}_{23}$, between native and denatured states of proteins in 1*M* osmolyte calculated from transfer free energies. The data were calculated from Eqs. (14) and (15) using the transfer model.[8] Partial molar volume changes of the protein ($-\Delta_N^D\overline{v}_2$) have been neglected, which leads to an error in the order of the size of the symbols (see text). The slopes of the fits are equal to the ratio of the volume fractions of osmolyte to water, $-\phi_3/\phi_1$, at 1*M* osmolyte [Eq. (16)]. The second quadrant (II) corresponds to stabilization, the fourth quadrant (IV) to destabilization. TMAO = ○, sarcosine = □, glycine betaine = ◇, proline = ⊡, glycerol = ◁, sorbitol = ▷, sucrose = △, trehalose = ▽, and urea = ×.

from 6 to 25 kDa. What is initially apparent is that values of $\Delta_N^D\mathcal{G}_{21}$ and $\Delta_N^D\mathcal{G}_{23}$ for protecting osmolytes fall in the upper left-hand quadrant (II), whereas those for the denaturing osmolyte urea fall in the lower right-hand quadrant (IV). These quadrants correspond, respectively, to stabilizing and destabilizing regions of solvation. For the protecting osmolytes in the second quadrant (II) there is a net accumulation of water to proteins and an exclusion of osmolyte from proteins upon unfolding, as is evident from the positive $\Delta_N^D\mathcal{G}_{21}$ and negative $\Delta_N^D\mathcal{G}_{23}$. As seen in the fourth quadrant (IV), urea binds more to denatured than to native proteins (positive $\Delta_N^D\mathcal{G}_{23}$) and water is more excluded (negative $\Delta_N^D\mathcal{G}_{21}$). The figure emphasizes that a solvent exchange occurs as the protein folds and unfolds, as expected.[11,76] Enrichment of water in the vicinity of the protein leads to an exclusion of osmolytes, and vice versa.

Second, given negligible denaturational volume changes $\Delta_N^D\overline{v}_2$, $\Delta_N^D\mathcal{G}_{21}$, and $\Delta_N^D\mathcal{G}_{23}$ at 1*M* osmolyte are 100% correlated and the slope is obtained using Eqs. (14) and (15):

$$\frac{\Delta_N^D\mathcal{G}_{21}}{\Delta_N^D\mathcal{G}_{23}} \approx \frac{\Delta_N^D\mathcal{G}_{21}+\Delta_N^D\overline{v}_2}{\Delta_N^D\mathcal{G}_{23}+\Delta_N^D\overline{v}_2} = \frac{c_3\overline{v}_3}{c_3\overline{v}_3-1} = -\frac{\phi_3}{\phi_1}. \qquad (16)$$

Equation (16) shows that the solvent exchange that accompanies denaturant-induced unfolding or osmolyte induced folding of proteins will always be determined by the ratio of the volume fractions of the solvent components in solution. Small deviations from a perfect correlation can occur, if changes in solution density around the protein occur upon unfolding ($\Delta_N^D\overline{v}_2 \neq 0$). Since the solution density, ρ, and osmolyte partial molar volumes, $\overline{v}_3$, are known, one can calculate the molarity, c_1, and partial molar volume, $\overline{v}_1$, of water, Eqs. (1) and (2); see Table I. These quantities allow for the calculation of solvation numbers of water molecules exchanged per osmolyte molecule that becomes either bound or excluded upon denaturation

$$\frac{\Delta_N^D N_{21}}{\Delta_N^D N_{23}} = \frac{c_1\Delta_N^D\mathcal{G}_{21}}{c_3\Delta_N^D\mathcal{G}_{23}} \approx -\frac{\overline{v}_3}{\overline{v}_1}, \qquad (17)$$

where Eq. (16) was used in the last step. The results of Eqs. (16) and (17) are given in Table V. The results of Figure 4 and Table V show the number of water molecules per osmolyte molecule that are exchanged when a protein folds/unfolds in the presence of 1*M* osmolyte. For example, for every two molecules of urea that bind to the protein, five molecules of water must be released; for every molecule of TMAO that is excluded from the protein, about four molecules of water must hydrate the protein; and for every saccharide molecule that is excluded, about 12 molecules of water must hydrate the protein. Similar considerations have recently been done by Smith and coworkers.[75]

The reason that $\Delta_N^D\overline{v}_2$ can be neglected in these consideration is that we are dealing with differences, specifically small differences between large numbers. Considering absolute solvation values $\mathcal{G}_{21}$ and $\mathcal{G}_{23}$ rather than differences, makes it necessary to account for $\overline{v}_2$. Figure 5 illustrates how important volume terms are when abso-

Table V

Solvent Exchange for the Native to Denatured Transition of Proteins in 1*M* Osmolyte at 25°C

1*M* osmolyte	Volume fraction ratio $-\frac{\phi_3}{\phi_1}$	Solvent exchange $-\frac{\overline{v}_3}{\overline{v}_1}\left(\#\frac{\text{waters}}{\text{osmolyte}}\right)$
TMAO	0.07670	3.94
Sarcosine	0.07151	3.70
Betaine	0.10895	5.43
Proline	0.09327	4.73
Glycerol	0.07841	4.03
Sorbitol	0.14032	6.83
Sucrose	0.27329	11.90
Trehalose	0.27541	12.10
Urea	0.04738	2.51

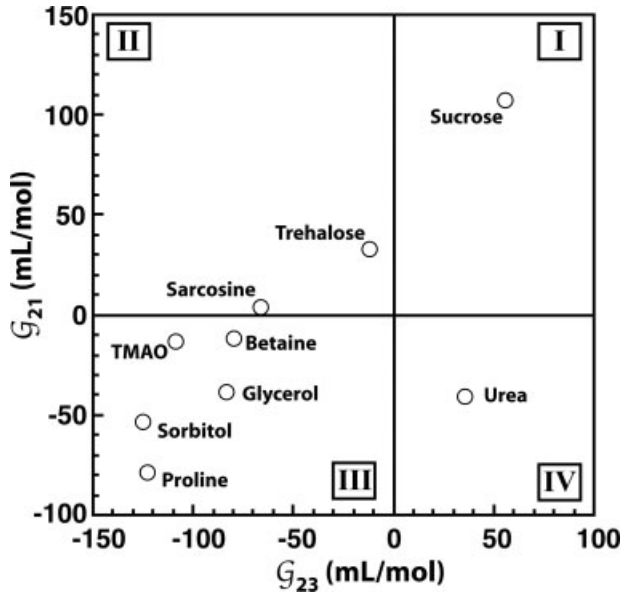

Figure 5

Hydration $\mathcal{G}_{21}$ versus osmolation $\mathcal{G}_{23}$ of the peptide group in 1*M* of different osmolytes. The data are replotted from Figure 2.

lute solvation values are calculated. The large contribution of $\overline{v}_2$ shifts the Kirkwood-Buff integrals of the peptide group in the presence of most osmolytes into the upper right and lower left quadrants (I) and (III). This is in stark contrast to the results with *differences* of Kirkwood-Buff integrals shown in Figure 4, where the data are exclusively in the other two quadrants (II) and (IV).

Note, that most points in Figure 5 are in the lower left quadrant (III). This is expected, because both water and osmolyte molecules cannot overlap with the atoms of the peptide group, and thus should be excluded. That means, both $\mathcal{G}_{21}$ and $\mathcal{G}_{23}$ should be negative, as observed. Only in cases in which the density of osmolyte around the peptide group is increased sufficiently to overcompensate this volume exclusion is $\mathcal{G}_{23}$ positive, as is the case for urea and sucrose. The same holds analogously for the hydration $\mathcal{G}_{21}$, which is positive in the case of sarcosine, trehalose, and sucrose.

CONCLUSIONS

Understanding the effect of cosolutes, especially osmolytes, on protein stability has been an issue of long standing. Our recent success in quantifying these effects in terms of the energetics of individual chemical entities on the protein surface[8,10] opened the opportunity to obtain a detailed structural resolution of the folding/unfolding energetics. Our approach is consistent with the earlier findings that favorable and unfavorable interactions of osmolytes with the peptide back bone or amide groups play a dominant role in osmolyte-dependent protein stability,[6,8,10,78–80] and it adds a wealth of information on other protein groups, as well as other osmolytes. We have combined this spatial resolution of the energetics with Kirkwood-Buff theory[15,16] to obtain, separately, the individual contributions of water and osmolytes.

Some of our current results are in line with previous findings. Hydration effects in osmolyte solutions are normally small and scaling with the size of the hydrated entity, independently of its chemical identity, whereas osmolation effects are highly variable.[64,81] We confirmed this trend for the solvation of the amino acids, where the hydration mostly depends on the amino acid size (bold line in Fig. 3). Amino acid osmolation, however, covers a broad range, demonstrating that compound-specific effects originate from the osmolyte–amino acid interaction.

Solvation changes upon protein unfolding are accompanied by very small volume effects. This leads to the classical exchange behavior,[11,77] in which enrichment of water at the protein surface leads to exclusion of osmolyte, and vice versa [see Eqs. (16) and (17)]. Such classical exclusion is manifested in Figure 4. Only the upper left and lower right quadrant are occupied, that is, hydration and osmolation changes have opposite signs: osmolyte and water mutually exclude each other. In addition, solvation effects on protein stability stem mostly from osmolation, not hydration: the magnitude of the denaturational change in hydration, $\Delta_N^D \mathcal{G}_{PW}$, is by an order of magnitude smaller than the change in osmolation, $\Delta_N^D \mathcal{G}_{PO}$.

We find the peptide backbone solvation to be surprisingly different from both the amino acid solvation and the overall protein solvation change upon unfolding. Highly variable amounts of solution compaction occur around peptide groups, so that even the backbone hydration strongly varies among different osmolyte solutions (Fig. 2). This is manifested in the lack of a classical exchange behavior seen in Figure 5, where mostly the upper right and lower left quadrant are occupied. Consequently, peptide groups tend to either exclude both osmolyte and water or to enrich both of them. Only urea shows the classical exchange behavior normally thought to be associated with preferential interactions.[11] Urea is enriched around backbone, whereas water is excluded (Fig. 2).

An especially remarkable finding is that sucrose is enriched around peptide backbone (Fig. 2). Normally, sucrose would be expected to be excluded, based on its large size and the net preferential hydration found for sucrose.[82] We find that this net preferential hydration is in fact caused by an accumulation of water that exceeds the accumulation of sucrose rather than water excluding sucrose.

Overall, these results give a much deepened insight into the solvation effects that govern the stability of proteins in osmolyte solutions.

REFERENCES

1. Yancey PH, Clark ME, Hand SC, Bowlus RD, Somero GN. Living with water stress: evolution of osmolyte systems. Science 1982;217: 1214–1222.
2. Hochachka PW, Somero GN. Biochemical adaptation: mechanism and process in physiological evolution. New York: Oxford University Press; 2002.
3. Pace CN. The stability of globular proteins. CRC Crit Rev Biochem 1975;3:1–43.
4. Pace CN, Grimsley G, Scholtz JM. Denaturation of proteins by urea and guanidine hydrochloride. In: Buchner J, Kiefhaber T, editors. Protein folding handbook. Weinheim, Germany: WILEY-VCH Verlag GmbH KGaA; 2004. Chapter 3.
5. Lin TY, Timasheff SN. Why do some organisms use a urea-methylamine mixture as osmolyte? Thermodynamic compensation of urea and trimethylamine *N*-oxide interactions with protein. Biochemistry 1994;33:12695–12701.
6. Bolen DW, Baskakov IV. The osmophobic effect: natural selection of a thermodynamic force in protein folding. J Mol Biol 2001; 310:955–963.
7. Nozaki Y, Tanford C. The solubility of amino acids and related compounds in aqueous urea solutions. J Biol Chem 1963;238:4074–4081.
8. Auton M, Bolen DW. Predicting the energetics of osmolyte-induced protein folding/unfolding. Proc Natl Acad Sci USA 2005;102:15065–15068.
9. Auton M, Bolen DW. Application of the transfer model to understand how naturally occurring osmolytes affect protein stability. Methods Enzymol 2007;428:397–418.
10. Auton M, Holthauzen LM, Bolen DW. Anatomy of energetic changes accompanying urea-induced protein denaturation. Proc Natl Acad Sci USA 2007;104:15317–15322.
11. Schellman JA. The thermodynamics of solvent exchange. Biopolymers 1994;34:1015–1026.
12. Zhang W, Capp MW, Bond JP, Anderson CF, Record MTJ. Thermodynamic characterization of interactions of native bovine serum albumin with highly excluded (glycine betaine) and moderately accumulated (urea) solutes by a novel application of vapor pressure osmometry. Biochemistry 1996;35:10506–10516.
13. Parsegian VA, Rand RP, Rau DC. Macromolecules and water: probing with osmotic stress. Methods Enzymol 1995;259:43–94.
14. Eisenberg H. Protein and nucleic acid hydration and cosolvent interactions: establishment of reliable baseline values at high cosolvent concentrations. Biophys Chem 1994;53:57–68.
15. Kirkwood JG, Buff FP. The statistical mechanical theory of solutions. J Chem Phys 1951;19:774–777.
16. Ben-Naim A. Inversion of Kirkwood-Buff theory of solutions—application to water-ethanol system. J Chem Phys 1977;67:4884–4890.
17. Ben-Naim A. Theory of preferential solvation of nonelectrolytes. Cell Biophysics 1988;12:255–269.
18. Chitra R, Smith PE. Preferential interactions of cosolvents with hydrophobic solutes. J Phys Chem B 2001;105:11513–11522.
19. Chitra R, Smith PE. Molecular association in solution: a Kirkwood-Buff analysis of sodium chloride, ammonium sulfate, guanidinium chloride, urea, and 2,2,2-trifluoroethanol in water. J Phys Chem B 2002;106:1491–1500.
20. Weerasinghe S, Smith PE. Cavity formation and preferential interactions in urea solutions: dependence on urea aggregation. J Chem Phys 2003;118:5901–5910.
21. Smith PE. Cosolvent interactions with biomolecules: relating computer simulation data to experimental thermodynamic data. J Phys Chem B 2004;108:18716–18724.
22. Abui M, Smith PE. A combined simulation and Kirkwood-Buff approach to quantify cosolvent effects on the conformational preferences of peptides in solution. J Phys Chem B 2004;108:7382–7388.
23. Smith PE. Local chemical potential equalization model for cosolvent effects on biomolecular equilibria. J Phys Chem B 2004;108: 16271–16278.
24. Smith PE. Protein volume changes on cosolvent denaturation. Biophys Chem 2005;113:299–302.
25. Smith PE. Chemical potential derivatives and preferential interaction parameters in biological systems from Kirkwood-Buff theory. Biophys J 2006;91:849–856.
26. Smith PE. Equilibrium dialysis data and the relationships between preferential interaction parameters for biological systems in terms of Kirkwood-Buff integrals. J Phys Chem B 2006;110:2862–2868.
27. Shimizu S. Estimating hydration changes upon biomolecular reactions from osmotic stress, high pressure, and preferential hydration experiments. Proc Natl Acad Sci USA 2004;101:1195–1199.
28. Shimizu S. Estimation of excess solvation numbers of water and cosolvents from preferential interaction and volumetric experiments. J Chem Phys 2004;120:4989–4990.
29. Shimizu S, Boon CL. The Kirkwood-Buff theory and the effect of cosolvents on biochemical reactions. J Chem Phys 2004;121:9147–9155.
30. Shimizu S, McLaren WM, Matubayasi N. The Hofmeister series and protein-salt interactions. J Chem Phys 2006;124:234905.
31. Shimizu S, Matubayasi N. Preferential hydration of proteins: a Kirkwood-Buff approach. Chem Phys Let 2006;420:518–522.
32. Russo AT, Rösgen J, Bolen DW. Osmolyte effects on kinetics of Fkbp12 C22A folding coupled with prolyl isomerization. J Mol Biol 2003;330:851–866.
33. Auton M, Bolen DW. Additive transfer free energies of the peptide backbone unit that are independent of the model compound and the choice of concentration scale. Biochemistry 2004;43:1329–1342.
34. Rösgen J, Pettitt BM, Bolen DW. Uncovering the basis for nonideal behavior of biological molecules. Biochemistry 2004;43:14472–14484.
35. Xie G, Timasheff SN. The thermodynamic mechanism of protein stabilization by trehalose. Biophys Chem 1997;64:25–43.
36. Liu Y, Bolen DW. The peptide backbone plays a dominant role in protein stabilization by naturally occurring osmolytes. Biochemistry 1995;34:12884–12891.
37. Qu Y, Bolen CL, Bolen DW. Osmolyte-driven contraction of a random coil protein. Proc Natl Acad Sci USA 1998;95:9268–9273.
38. Wang A, Bolen DW. A naturally occurring protective system in urea-rich cells: mechanism of osmolyte protection of proteins against urea denaturation. Biochemistry 1997;36:9101–9108.
39. Høiland H. Partial molal volumes of biochemical model compounds in aqueous solution. In: Hinz H-J, editor. Thermodynamic data for biochemistry and biotechnology. New York: Springer-Verlag; 1986. Chapter 2.
40. Lee B, Richards FM. The interpretation of protein structures: estimation of static accessibility. J Mol Biol 1971;55:379–400.
41. Lesser GJ, Rose GD. Hydrophobicity of amino acid subgroups in Proteins. Proteins 1990;8:6–13.
42. Schellman JA. Protein stability in mixed solvents: a balance of contact interaction and excluded volume. Biophys J 2003;85:108–125.
43. Creamer TP, Srinivasan R, Rose GD. Modeling unfolded states of peptides and proteins. Biochemistry 1995;34:16245–16250.
44. Creamer TP, Srinivasan R, Rose GD. Modeling unfolded states of proteins and peptides. II. Backbone solvent accessibility. Biochemistry 1997;36:2832–2835.
45. Caron A, Palenik GJ, Goldish E, Donohue J. The molecular and crystal structure of trimethylamine oxide, $(CH_3)_3NO$. Acta Crystallogr 1964;17:102–108.
46. Kayushina RL, Vainshtein BK. Rentgenografiye. Opredepenie strukturi L-prolina. Kristallografiya 1965;10:833–844.

47. van Koningsveld H. The crystal structure of glycerol and its conformation. Rec Trav Chim Pays-Bas 1968;87:243–254.
48. Brown GM, Rohrer DC, Berking B, Beevers CA, Gould RO, Simpson R. The crystal structure of α,α-trehalose dihydrate from three independent X-ray determinations. Acta Crystallogr, Sect B 1972;28.B:3145–3158.
49. Hanson JC, Sieker LC, Jensen LH. Sucrose: X-ray refinement and comparison with neutron refinement. Acta Crystallogr, Sect B 1973;29.B:797–808.
50. Bhattacharyya SC, Saha NN. Crystal and molecular-structure of sarcosine hydrochloride. J Cryst Mol Struct 1978;8.3:105–113.
51. Mak TCW. Crystal structure of betaine monohydrate, $(CH_3)_3NCH_2COO\text{-}H_2O$. J Mol Struct 1990;220:13–18.
52. Schouten A, Kanters JA, Kroon J, Comini S, Looten P, Mathlouthi M. Conformational polymorphism of D-sorbitol (D-glucitol): The crystal and molecular structures of D-glucitol 2/3-hydrate and epsilon D-glucitol. Carbohydr Res 1998;312.3: 131–137.
53. Zavodnik V, Stash A, Tsirelson V, de Vries RY, Feil D. Electron density study of urea using Tds-corrected X-ray diffraction data: Quantitative comparison of experimental and theoretical results. Acta Crystallogr, Sect B 1999; 55.B:45–54.
54. Allen FH. The cambridge structural database: A quarter of a million crystal structures and rising. Acta Cryst 2002;B58:380–388.
55. Taverner BC. Improved algorithm for accurate computation of molecular solid angles. J Comput Chem 1996;17:1612–1623.
56. Koradi R, Billeter M, Wuthrich K. Molmol: a program for display and analysis of macromolecular structures. J Mol Graph 1996;14: 51–55.
57. Wu P, Bolen DW. Osmolyte-induced protein folding free energy changes. Proteins 2006;63:290–296.
58. Zweifel ME, Leahy DJ, Hughson FM, Barrick D. Structure and stability of the ankyrin domain of the *Drosophila* notch receptor. Protein Sci 2003;12:2622–2632.
59. Holthauzen LM, Bolen DW. Mixed osmolytes: the degree to which one osmolyte affects the protein stabilizing ability of another. Protein Sci 2007;16:293–298.
60. Santoro MM, Bolen DW. Unfolding free energy changes determined by the linear extrapolation method. I. Unfolding of phenylmethanesulfonyl alpha-chymotrypsin using different denaturants. Biochemistry 1988;27:8063–8068.
61. Bolen DW, Santoro MM. Unfolding free energy changes determined by the linear extrapolation method. II. Incorporation of delta G degrees N-U values in a thermodynamic cycle. Biochemistry 1988; 27:8069–8074.
62. Makhatadze GI. Thermodynamics of protein interactions with urea and guanidinium hydrochloride. J Phys Chem B 1999;103:4781–4785.
63. Ben-Naim A. Statistical thermodynamics for chemists and biochemists. New York: Plenum Press; 1992.
64. Rösgen J, Pettitt BM, Bolen DW. Protein folding, stability, and solvation structure in osmolyte solutions. Biophys J 2005;44:16896–16911.
65. Ferreon AC, Ferreon JC, Bolen D, Rösgen J. Protein phase diagrams. II. Non-ideal behavior of biochemical reactions in the presence of osmolytes. Biophys J 2006;92:245–256.
66. Makhatadze GI, Privalov PL. Heat capacity of proteins. I. Partial molar heat capacity of individual amino acid residues in aqueous solution: hydration effect. J Mol Biol 1990;213:375–384.
67. Privalov PL, Makhatadze GI. Heat capacity of proteins. II. Partial molar heat capacity of the unfolded polypeptide chain of proteins: protein unfolding effects. J Mol Biol 1990;213:385–391.
68. Hackel M, Hedwig GR, Hin HJ. The partial molar heat capacity and volume of the peptide backbone group of proteins in aqueous solution. Biophys Chem 1998;73:163–177.
69. Hackel M, Hinz HJ, Hedwig GR. A new set of peptide-based group heat capacities for use in protein stability calculations. J Mol Biol 1999;291:197–213.
70. Hackel M, Hinz HJ, Hedwig GR. Partial molar volumes of proteins: amino acid side-chain contributions derived from the partial molar volumes of some tripeptides over the temperature range 10–90 °C. Biophys Chem 1999;82:35–50.
71. Hedwig GR, Hinz HJ. Group additivity schemes for the calculation of the partial molar heat capacities and volumes of unfolded proteins in aqueous solution. Biophys Chem 2003;100:239–260.
72. Chalikian TV. Volumetric properties of proteins. Annu Rev Biophys Biomol Struct 2003;32:207–235.
73. Lin LN, Brandts JF, Brandts JM, Plotnikov V. Determination of the volumetric properties of proteins and other solutes using pressure perturbation calorimetry. Anal Biochem 2002;302:144–160.
74. Royer CA. Revisiting volume changes in pressure-induced protein unfolding. Biochim Biophys Acta 2002;1595:201–209.
75. Rösgen J, Hinz HJ. Response functions of proteins. Biophys Chem 2000;83:61–71.
76. Schellman JA. Fifty years of solvent denaturation. Biophys Chem 2002;96:91–101.
77. Pierce V, Kang M, Aburi M, Weerasinghe S, Smith PE. Recent applications of Kirkwood-Buff theory to biological systems. Cell Biochem Biophys 2008;50:1–22.
78. Scholtz JM, Barrick D, York EJ, Stewart JM, Baldwin RL. Urea unfolding of peptide helices as a model for interpreting protein unfolding. Proc Natl Acad Sci USA 1995;92:185–89.
79. Cannon JG, Anderson CF, Record MTJ. Urea-amide preferential interactions in water: quantitative comparison of model compound data with biopolymer results using water accessible surface areas. J Phys Chem B 2007;111:9675–9685.
80. Hong J, Capp MW, Saecker RM, Record MTJ. Use of urea and glycine betaine to quantify coupled folding and probe the burial of DNA phosphates in lac repressor-lac operator binding. Biochemistry 2005;44:16896–16911.
81. Rösgen J, Pettitt BM, Bolen DW. An analysis of the molecular origin of osmolyte-dependent protein stability. Protein Sci 2007;16: 733–743.
82. Lee JC, Timasheff SN. The stabilization of proteins by sucrose. J Biol Chem 1981;256:7193–7201.